# Journal of Materials Chemistry C

Accepted Manuscript


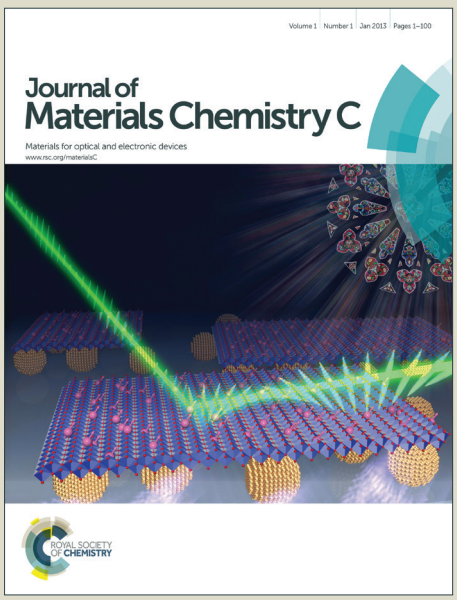





ROYAL SOCIETY OF CHEMISTRY

www.rsc.org/materialsC

# Can a metal nanoparticles based catalyst drive the selective growth of bright SiV color centers in CVD diamonds?

*Ilaria Cianchetta, Massimo Tomellini, Emanuela Tamburri, Stefano Gay, Dario Porchetta, Maria Letizia Terranova, Silvia Orlanducci**

Dip.to di Scienze & Tecnologie Chimiche - MinimaLab, Università di Roma ‘‘Tor Vergata’’ Via Della Ricerca Scientifica, 00133 Rome (Italy)
E-mail: silvia.orlanducci@uniroma2.it

## Abstract

We propose an efficient catalytic method based on nickel nanoparticles to produce a massive amount of Si color centers in diamonds directly during the CVD growth. A thermodynamic model was firstly developed to describe the mechanism of the Si inclusion in diamonds and a subsequent series of diamond syntheses was carried out to corroborate the model. Raman and photoluminescence spectroscopy as well as electron microscopy were used to characterize the diamond samples. All the treatments with Ni nanoparticles were able to produce diamond samples with a Si related fluorescence intensity higher than the one related to the un-treated samples. Finally a critical discussion of our results, in comparison with the ones reported in literature, is presented.

## 1. Introduction

Diamonds with high structural and compositional purity are not as interesting as diamonds hosting few little defects (*i.e.* point defects). These point defects, called with the self-explaining name “color centers”, display remarkable optical properties and their study represents, nowadays, a very hot topic in quantum optics. In particular, many of these diamond defects have been proposed as single-photon sources for several applications, ranging from information processing, cryptography, spin-based qubit in quantum computing and metrology.[1-4] Furthermore, fluorescent diamonds have generated a great interest for biological applications, thanks to the biocompatibility of diamond/$sp^3$ crystalline carbon and

the stability and tunability of the related emission.[5-8] Up to now, the attention has been mostly directed towards the nitrogen color centers (NV centers) either naturally found in diamonds or produced by means of proton irradiation. The NV center, though, is no longer considered the optimal candidate, especially for the labeling of biological targets. Its relatively long photoluminescence lifetime and the broad emission band in the green region of the visible spectrum, often overlaps with the natural fluorescence of biological objects resulting inefficient for imaging purposes. The recently studied nickel, chromium[9-10] and, above all, silicon color centers are now considered better candidates for biological and single photon source applications, thanks to their narrow fluorescence emission in the red and NIR part of the electromagnetic spectrum. The fluorescence of the silicon vacancy (SiV) complex was first observed in 1981 by Vavilov *et al.*,[11] but it was unambiguously verified to involve silicon impurities only in 1995.[12] The first theoretical model of a silicon-vacancy complex was proposed by Goss *et al.*[13] but, so far, electronic level scheme, geometry and dynamics population of the SiV center are still under investigation.[14-18]

The silicon related color center photoluminescence (PL) spectrum consists of a sharp zero phonon line (ZPL) at 738 nm, with a full width at half maximum FWHM of few nanometers, a weak vibronic sidebands at room temperature, and a short photoluminescence lifetime of 1–4 ns.[19,20]

Despite the deep interest of the scientific community in these fluorescent defects, the controlled formation of color centers in diamond is still a challenge. The most used technique for the production of color centers is ion implantation followed by the annealing of the diamond crystal.[21,22] Regardless the undoubted progresses of this technique, this synthetic route is not yet efficient in producing systems with high fluorescence intensity. A severe deterioration of the diamond lattice is observed for large ion dosage, with the consequent formation of amorphous and graphitic carbon, responsible for the fluorescence quenching.

In order to avoid the lattice damages caused by proton irradiation and obtain diamonds with low structural defects the ultimate solution would be the direct inclusion of color centers during the growth of the diamond lattice. The CVD process represents a viable route for the formation of good crystalline quality diamonds and, as previously reported,[12] the inclusion of SiV centers is often found in CVD diamonds. This side effect is due to the presence of Si atoms in the CVD chamber originating from the plasma chemical etching of the exposed Si substrates and/or fused silica components of the CVD reactor. The major drawback of this fabrication method is the unpredictability of the amount of the SiV centers inclusions. As a consequence, diamond materials with uncontrolled luminescent properties are typically formed. Some improvements have been obtained using nondeterministic silicon precursors, such as silane or silicon nanoparticles (NP).[24,25] In particular, by using silane, it was demonstrated that the PL intensity strongly depends on the $SiH_4/CH_4$ ratio, obtaining the best result at low $SiH_4$ concentration. The increasing of the gas ratio leads, instead, to the formation of structural defects which resolve in a nonradiative recombination and a strong decreasing of the PL intensity.[24] Conversely, the use of Si NP drives the formation of bright fluorescent diamonds matrices but embedded Si NP are also found[25,26]. Anyway, both these methods are in principle not able to generate spatially localized SiV.

With the aim to develop innovative methods for producing bright and localized SiV in diamonds, the authors of this paper wondered whether nanotechnology can provide a valid assistance to overcome the synthetic constrains so far encountered, and establish a theoretical and experimental approach to positively answer to the question given in the title.

The idea is to create a massive amount of color centers by inducing the inclusion of foreign atoms into the diamond lattice by means of the same mechanism which enables the growth of diamond crystals *via* CVD. In this view, assuming that diffusion processes are forbidden in the diamond lattice, the formation of SiV would be due to the substitution of a C atom by a Si atom present in the gaseous phase of the CVD chamber during the crystal growth.

Therefore, with the addition of a localized and efficient source of Si gas, the SiV inclusion into diamond would be improved without inducing structural damages.

The role of Si-gas phase localized source is played by a Si substrate patterned with nickel nanoparticles (NiNP). The efficiency of the NiNP to promote the formation of silicon gaseous species is related to the formation of silicide, as demonstrated in the following theoretical background section, with lower surface energy compared to the bare silicon substrate. Subsequently, silicides react with H to form gaseous species, whose concentration depends on the Ni particles radius and is so much higher as smaller the Ni particles size.

The theoretical model and an innovative synthetic strategy for the controlled generation of massive SiV centers in diamonds is accurately described in the paper.

The fluorescence intensity of diamonds grown using NiNP catalysts is discussed and compared to the fluorescence intensity of CVD diamond already reported in literature. It is found that NiNP strongly improve the occurrence of SiV defects in the diamond lattice, allowing to obtain diamonds more than one order of magnitude (brighter than those already observed.

## 2. **Theoretical backgroung**

The diamond growth by CVD synthesis is a well-known process involving the decomposition of a gaseous mixture containing a small quantity of hydrocarbon in excess of hydrogen. The typical mixture composition is 1% $CH_4$ in $H_2$. Analysis of the composition and of the gas-surface reactions have been deeply investigated[27,28] and a kinetic model for diamond nucleation has been proposed[29].

In the framework of such model, the growth of a diamond crystal is well described by several surface reactions one of them is the addiction of a methyl group to a surface radical leading to

the diamond growth; Reaction (1) describes The formation, in the gas phase, of the methyl radicals, that are the principal growing specie:[27]

$$CH_4 + H = CH_3 + H_2 \qquad (1)$$

Provided the presence of a silicon gaseous phase and/or the presence of $SiH_x$ radicals in the CVD chamber, the insclusion of Si atoms during the C lattice growth determines the formation of the color centers. As already reported in the introduction the use of a gaseous mixture of $SiH_4$ and $CH_4$ , has already been proposed[24], but it was also demonstrated that concentrations higher than 0.08% ($SiH_4/CH_4$ %) affect the diamond crystal structure,therefore an alternative route is necessary to provide a massive formation of SiV and good crystalline diamonds.

An alternative approach is represented by the controlled exploitation of the silicon susbtrate as silane precursor. The hydrogen etching leads to the formation of silicon gaseous species, in first approximation silane and $SiH_x$ radicals,[30,31] according to the following reaction (2)

$$Si + 4H = SiH_4 \qquad (2)$$

At the equilibrium, the equivalence between the chemical potential of the products, silane in this case, and the chemical potentials of the reactants (silicon in the bulk solid phase and atomic hydrogen) holds:

$$\mu^0_{SiH_4} + k_B T \ln P_{SiH_4} = \mu^0_{Si} + 4\left(\mu^0_H + k_B T \ln P_H\right) \quad (3)$$

Defining, for the chemical reaction (2), the reaction constant $K_e$ as a function of the standard chemical potential:

$$K_e = e^{-\left(\frac{\mu^0_{SiH_4} - \mu^0_{Si} - 4\mu^0_H}{k_B T}\right)} \qquad (4)$$

it is possible to rewrite eq.3 as

$$k_B T \ln K_e = k_B T \ln P_{SiH_4} - 4k_B T \ln P_H \qquad (5)$$

and to express the $SiH_4$ pressure in the synthesis chamber as a function of the $K_e$ constant and of the hydrogen pressure

$$P_{SiH_4} = K_e P_H \qquad (6)$$

In the synthesis chamber $SiH_4$ is subjected to decomposition and adsorption reactions analogously to methane. As the methyl radical, hydrogenated silicon radicals can saturate the dangling bonds of the forming diamond surface.[30,32] The subsequent rearrangement of carbon atoms around the foreign atom during the crystal formation is supposed to be the driving force for the inclusion of the vacancies and the creation of the Si related color center.

This mechanism can explain the formation of silicon related defects, often found in CVD diamonds grown on silicon substrates or in the presence of silicon-based components of reactors.

In order to promote the formation of silicon gaseous species, a substrate treatment able to lower the surface energy of the silicon wafer and to weaken the Si-Si bond is decisive. The large Ni diffusion in silicon crystal and the subsequent formation of nickel silicides represent an accessible route to our goal, since it lowers the Si surface energy[33] and weakens, ultimately breaks, the Si-Si bonds.[34] We believe that the heterogeneous reaction between H atom and the silicon-nickel phase, at the nanometric scale, may facilitate the silicon etching with consequent inclusion during the diamond growth. In particular, NiSi and $NiSi_2$ are believed to be more likely formed under the diamond synthesis conditions and therefore adopted in the present work. Typically, the formation of NiSi occurs in a very large temperature window (400 – 700°C),[35] while the $NiSi_2$ formation is found at higher temperatures (>750 °C, for bulk material).[36-38] However, it is possible that the small size of the used NiNP allows the formation of $NiSi_2$ also in our conditions.[39-41]

The formation of gaseous silane in presence of NiSi species is reported in eq (7):

$$(NiSi_x)_{NP} + 4xH = xSiH_4 + Ni \qquad (7)$$

where the subscript "NP" indicates that the $NiSi_x$ in the "nanoparticle" phase and Ni in the solid phase on the silicon substrate surface. At the equilibrium the relation between the chemical potentials $\mu_k$ of all the species holds:

$$\mu_{NiSi_x} + 4x\mu_H = x\mu_{SiH_4} + \mu_{Ni} \quad (8)$$

In particular, $NiSi_x$ is considered to be a single component. Accordingly, the chemical potential of the silicide is written as[42, 43]

$$\mu_{NiSi_x} = \mu^0_{NiSi_x} + \frac{2\bar{\upsilon}\sigma}{R} \quad (9)$$

where $\mu^0_{NiSi_x}$ is the chemical potential of the "bulk" phase (*i.e.* in the limit of infinite size, $R \to \infty$ ) that is in its standard state. In eqn.12 $\sigma$ and $\bar{\upsilon}$ are the surface excess free energy and the molar volume of the silicide, respectively, and $R$ is the radius of the particle. Inserting eqn.12 in eqn.11 and specifying the chemical potential of the gas phase components, one obtains

$$x\left(\mu^0_{SiH_4} + k_BT\ln P^{(NP)}_{SiH_4}\right) + \mu^0_{Ni} = \mu^0_{NiSi_x} + \frac{2\bar{\upsilon}\sigma}{R} + 4x\left(\mu^0_H + k_BT\ln P^{(NP)}_H\right) \quad (10)$$

With $P_k$ denoting the partial pressure of the k-th component in the gas phase and the superscript (NP) to remind that the heterogeneous equilibrium involves a nanometric phase. By exploiting the equality $\mu^0_{NiSi_x} = \mu^0_{Ni} + x\mu^0_{Si}$ eqn.13 eventually leads to

$$x\left(\mu^0_{SiH_4} - \mu^0_{Si} - 4\mu^0_H\right) = \frac{2\bar{\upsilon}\sigma}{R} + xk_BT\ln\frac{P^{(NP)4}_H}{P^{(NP)}_{SiH_4}} \quad (11)$$

which becomes, taking into account eqn.9

$$-xk_BT\ln K_e = \frac{2\bar{\upsilon}\sigma}{R} + xk_BT\ln\frac{P^{(NP)4}_H}{P^{(NP)}_{SiH_4}} \quad (12)$$

or, alternatively,

$$\frac{P_{SiH_4}^{(NP)}}{P_{SiH_4}} = \left(\frac{P_H^{(NP)}}{P_H}\right)^4 e^{\frac{2\bar{\upsilon}\sigma}{xR}\frac{1}{k_B T}} \qquad (13)$$

We recall that the partial pressure values without superscripts refer to the equilibrium between gas and "bulk" silicide phases (eqns.2, 3). Under the approximation of invariant hydrogen pressure, eqn.13 shows that the $SiH_4$ pressure ratio scales as a function of both the particle radius and the chemical composition of the silicide. This ratio is positive, and increases with the decrease of $R$. The silicide reacts with H to form gaseous species of silicon (silane) to a major extent when/if the Si atoms are inside the NP rather than when they are bonded to the Si substrate surface, proving the $NiSi_x$ nanoparticles highly efficient silicon sources.

Before concluding this section, we briefly comment on another size-related effect, namely the melting of the catalyst particle. In fact, the melting temperature of a small particle is found to decrease with decreasing the particle radius. To be specific

$$\frac{T^{(NP)}}{T^*} = e^{-\frac{2\bar{\upsilon}\sigma}{\Delta HR}} \qquad (14)$$

where $\Delta H$ is the molar enthalpy change for the melting and $T^*$ is the melting temperature of the bulk system. Therefore, in the absence of detailed values of the physical quantities entering the expression above, the possibility that the nanoparticle is in a liquid state cannot be ruled out. However, we point out that, within the assumption of the model, the thermodynamic approach here developed can be applied to this case as well.

In order to experimentally verify this model, a set of different diamond samples was made and morphological, structural and photoluminescence studies are discussed in the last section.

## 3. Experimental

The Ni nanoparticles (NP) were synthesized by means a chemical reduction of the $Ni^{2+}$ ions resulting from an aqueous solution of 0.1 M $NiCl_2$ (Sigma-Aldrich). The immediate formation of a black flocculate of Ni nanoparticles is observed when $NaBH_4$ (Sigma-Aldrich) is added in excess to the $NiCl_2$ solution under stirring. The produced NP were then separated and purified by centrifugation and water washing. Successively, three dispersions at different concentration of Ni NP, *i.e.* I=$3x10^{-1}$M, II = $3x10^{-2}$M, III = $3x10^{-3}$M, were prepared. A fixed amount of 0.25 μm sized diamond grains paste (Metadi, Buehler) in acetone was added to each of the three NiNP dispersions. These dispersions were used to pre-treat slices of silicon wafers, used subsequently as substrates for the CVD diamond growth. The used protocol consists in an ultrasound treatment of the Si slices in the Ni + diamond dispersions for 15 minutes, followed by an ultrasonic cleaning in ethanol in order to remove the residues of the diamond paste or NiNP aggregate from the surface. However, this cleaning treatment do not completely eliminate the Ni NP from the Si substrate, as reveled from SEM and EDX analysis of the treated substrate reported in the supplementary information (figure S1). The residual Ni particles were thus exploited in the CVD process for the diamond growth.

The diamond synthesis was performed under the experimental conditions summarized in table 1 adopting procedures previously optimized.[44] In particular synthetic processes lasting one and two hours have been carried out for the purpose of studying the effect of NiNP both on diamond isolated grains and on diamond films.

Finally, in order to discriminate the effect of the Ni NP on the CVD growth process, diamond films and isolated crystals were also grown with the only use of diamond paste.

**Table 1:** Synthesis parameter for the CVD diamond growth

| Parameters | Value |
|---|---|
| Substrate-filament distance | 8 mm |

| | |
|---|---|
| Filament temperature | 2100°C |
| Substrate Temperature | 650°C |
| $H_2$ flux | 198 sccm |
| $CH_4$ flux | 2.5 sccm |
| Pressure | 36 Torr |
| Synthesis time | (1- 2) h |

The morphological characterization of the samples was performed by a field emission gun scanning electron microscope (FEG-SEM) Hitachi S-4000. In order to estimate size particles distribution and surface coverage, SEM images were analyzed using ImageJ as image analysis software.

Raman analyses were performed by menas of a micro-Raman setup equipped with a 514 nm Ar laser source, a liquid nitrogen cooled CCD detector and a Horiba iHR550 spectrometer. A Horiba Jobin Ivon Explora fluorescence microscope was used to acquire maps of the Raman signal and fluorescence spectra. In the latter case, a solid state laser source at 532 nm was used. The detector was an air cooled CCD device. The integrated spectrograph allowed a resolution of 1.2 $cm^{-1}$ with a spatial resolution in the xy plane < 1 μm.

The Raman spectra acquired for each sample were fitted with Lorentz curves. The crystal quality of the synthesized diamonds was estimated by the full width at half maximum (FWHM) of the first order diamond Raman peak at 1332 $cm^{-1}$,[45] that for a single crystal diamond is 0.13 nm. The inclusion of silicon defects is observed by the fluorescence analysis of the SiV peak at 738 nm. All the spectra are recorded using the same laser power and integration time. In order to evaluate the homogeneity of samples, more than 100 spectra were recorded and mediated.

## 4. Results and Discussion

The SEM images of diamond samples grown on Ni NP treated substrates obtained using the dispersions I, II and III are reported in Fig. 1

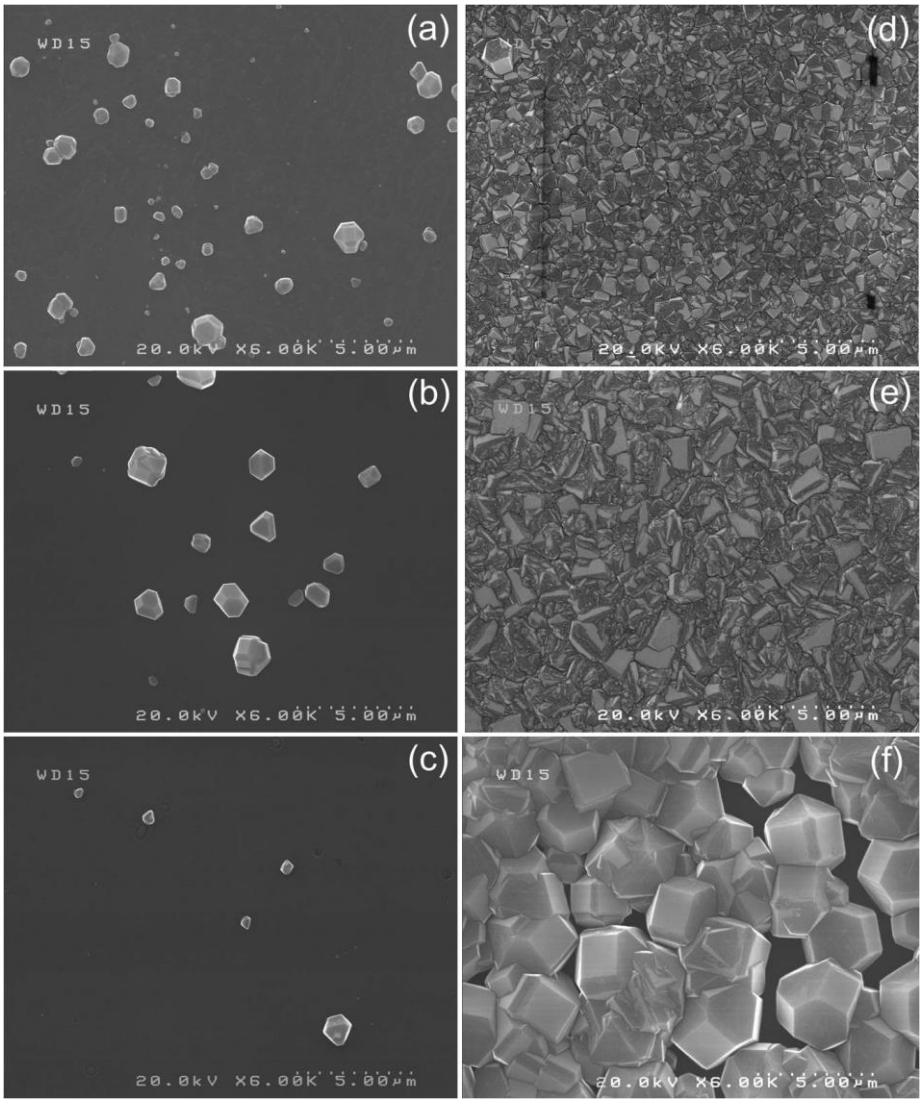


**Fig. 1:** SEM images of diamond samples grown using NiNP dispersion: (a) I, (b) II and (c) III for 1 hour of synthesis time and (d) I, (e) II, and (f) III for 2 hours of synthesis time.

In particular, the photos show the morphology of the samples prepared with: (a-b-c) 1 hour and (d-e-f) 2 hours of synthetic process. For all the samples, a homogeneous nucleation and a rapid growth are observed. The morphological analysis in term of surface coverage and crystal size are summarized in Tab. 2. For comparison, the table also reports the data related to typical diamond samples grown on Si substrates treated using only the diamond paste.

**Table 2:** Average grain size and surface coverage of diamond samples grown using Ni NP at different concentration and synthesis time. For comparison, the data related to diamond samples grown on Si substrates treated using only the diamond past are also reported.

| Ni NP concentration (M) | Synthesis Time (h) | Substrate Treatment | Grain Size (µm) | Surface Coverage (%) |
|---|---|---|---|---|
| 0 | 3 | Diamond paste 0.25 µm | 3 | 35% |
| 0 | 1 | UND seeds | < 1 | 100% |
| III: $3x10^{-3}$ | 1 | Ni NP | < 1 | 2% |
| II: $3x10^{-2}$ | 1 | Ni NP | 0.80 ↔1.2 | 11% |
| I: $3x10^{-1}$ | 1 | Ni NP | 0.80 ↔1.2 | 46% |
| III: $3x10^{-3}$ | 2 | Ni NP | >2 | 60% |
| II: $3x10^{-2}$ | 2 | Ni NP | continuous film | 100% |
| I: $3x10^{-1}$ | 2 | Ni NP | continuous film | 100% |

It is interesting to observe that, while three hours of synthesis process are required to get significative diamond coverage for the substrates treated with the only diamond paste 35%, a large amount of diamonds is instead produced within an1 hour in the presence of Ni NP (46% with Ni concentration of $3x10^{-1}$ M). Moreover, within only 2 hours a continuous diamond film is obtained, using a Ni dispersion $3x10^{-2}$ M.

For comparison diamond film growth by using ultra nonodiamond (UND) as seeds is already reported in the table 2. Noteworthy, the silicon color center related fluorescence was significantly observed in all the samples except for the diamond film grown by UND seeds.

The structural analysis of the samples was carried out by microRaman spectroscopy. The typical spectra are reported in Fig. 2.

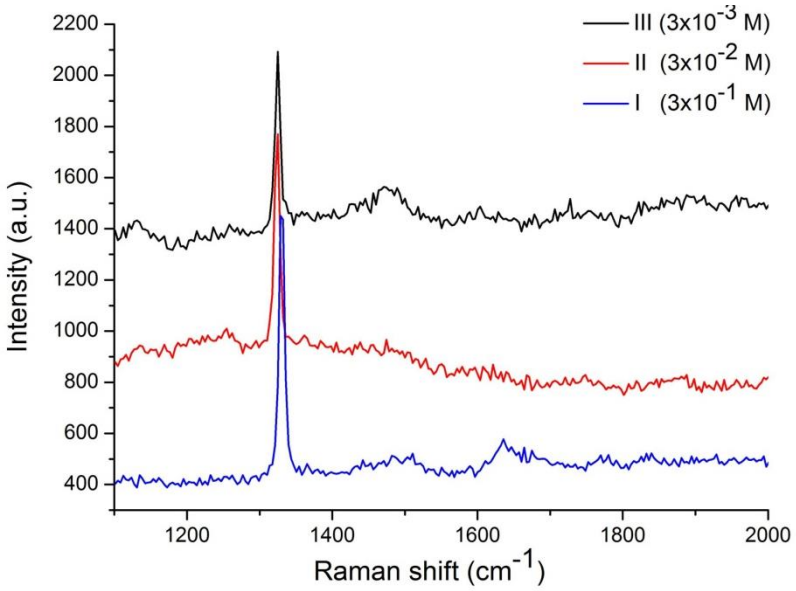


**Fig. 2**: Typical Raman spectra of samples grown using Ni NP at different concentrations and 1 hour of synthesis time

For all the samples treated with Ni NP, a very intense and sharp Raman peak was recorded. This result can be associated to a good quality of the diamond crystals. In particular, an increase of the intensity of the Raman peak and a decrease of the FWHM with increasing Ni concentration are observed. It is interesting to note that the Ni NP not only exhibit a catalytic effect on the nucleation and growth rate of diamond, but also allow the preservation, if not the improvement, of the crystalline quality. The little shift observed in first order diamond Raman peak for sample grown using Ni NP at the concentration of $3x10^{-1}$ M is mainly due to an increase of residual stress within the CVD diamonds.

The PL spectra, in the range 530-800 nm, of our synthetic diamonds are reported in the supplementary information (S.I.Figures 2-5), whereas the PL spectra in the 700-745 nm range are highlighted and reported in Fig. 3.

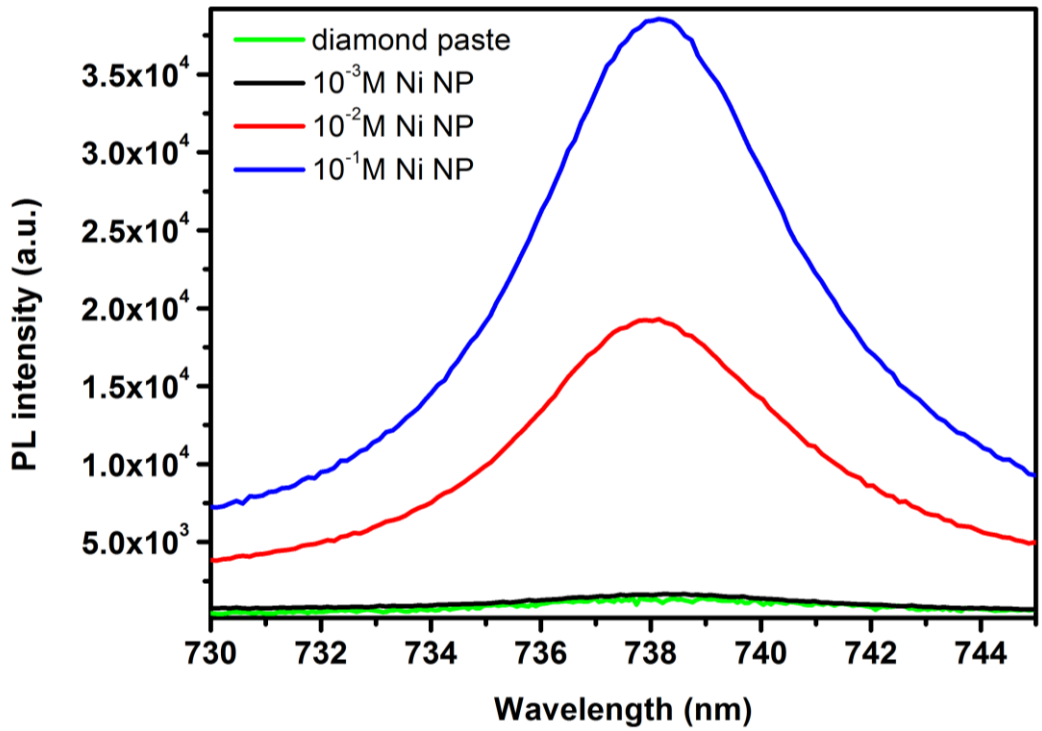


a)

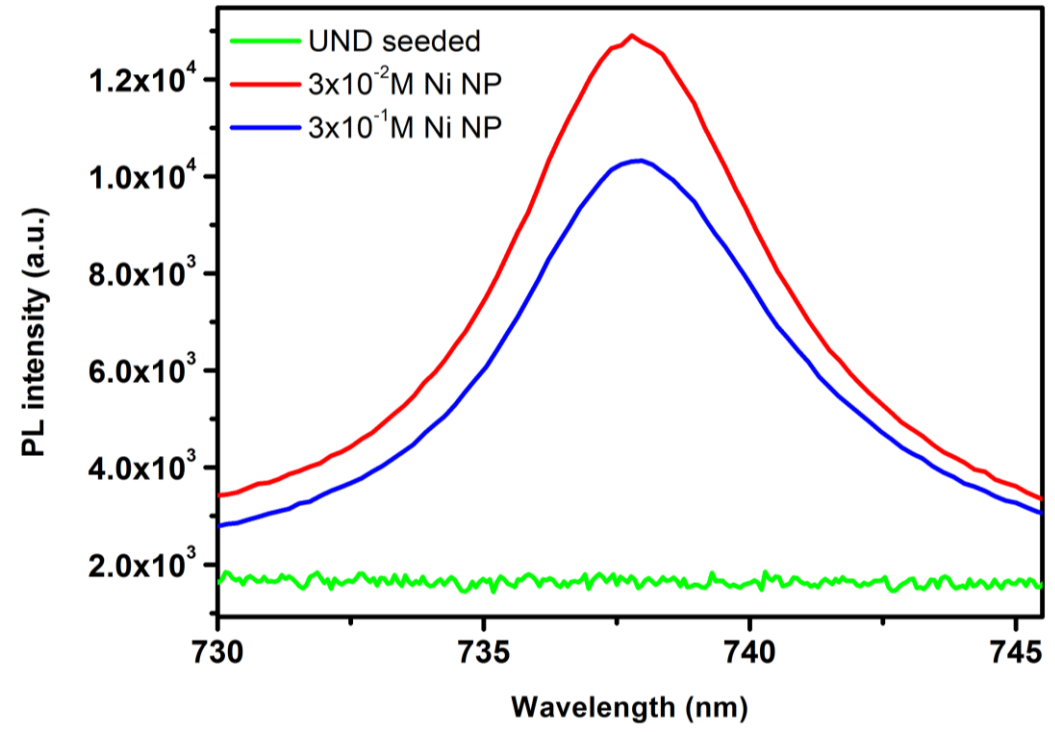


b)

**Fig. 3 a)** PL spectra of SiV center from diamonds grains grown on Si substrates treated with Ni NP and syinthesis time of 1 hour. The PL of CVD diamonds grains grown on Si substrate treated using only the diamond paste are also reported (green line); **b)** PL spectra of SiV

center from diamond films grown on Si substrates treated with Ni NP and syinthesis time of 2 hour (blue and red lines) and the PL of CVD diamonds film grown by using UND seeds (green line). The PL spectrum from the lower NiNP concentration is not reported in this figure because, as reported in table 2, the sample is not a continuos film.

In particular, fig. 3 (a) shows the PL of isolated diamond crystals obtained after 1 hour of synthesis. An increase of the SiV fluorescence emission is observed for samples treated with Ni NP. Notably, the sample treated with the dispersion I ($10^{-1}$ M, blue spectrum) shows a signal that is 20 times more intense than the un-treated diamonds.

The effect of the Ni concentration on the PL intensity, can be explained by considering that the deposition is not performed under equilibrium conditions, owing to the consumption of gaseous species by the growing diamond phase. On this basis, the model above discussed should be implemented by taking into account the differences between the chemical potentials of the reaction components above defined that is, the reaction affinity, $A$. The displacement from equilibrium under reactive conditions can therefore be modeled by means of the kinetic law of mass action. Accordingly, the reaction rate for a single NP is proportional to the reaction affinity, $A = \sum_i \nu_i \mu_i$, where $\nu_i$ is the stoichiometric coefficient of the i-th component. On the other hand, the total rate of the reaction is proportional to the surface density of NP which, in turn, is expected to increase with Ni concentration. As a consequence, the larger the rate of silane production the larger the availability of Si atoms able to generate SiV in CVD diamond.

Fig. 3 (b) shows the PL spectra of the diamond films obtained by the use ofthe Ni NP dispersions (blue and red spectra) and the UND seed (green spectrum). While no SiV related fluorescence is detected from the UND treated film, the highest fluorescence is observed from the film pretreated with the dispersion II ($10^{-2}$ M, blue spectrum).

This is not a surprising result because the growth of the film shields the substrate from etching, decreasing the formation of Si gaseous specied and the inclusion of Si in the diamond lattice. As a result the SiV are predominately located near the interface between diamond-Si substrate. As demonstrated by Donado and Dollingher the SiV signal in diamond films exhibits a strong decrease at a distance of 5 μm from the substrate-film interface and almost disappears at 10 μm.

As already discussed, the catalytic effect of the Ni NP dispersion determines a faster growth of the diamond, then a trade-off has to be found between the Ni NP concentration and the synthesis time for the highest fluorescent intensity from continuous films. In our conditions $10^{-2}$ M represents the optimal solution.

Being aware that a comparison between fluorescence intensities of diamond samples grown in different conditions, and collected by different set-up, is a challenging task, we would like to introduce here the ratio($I_{PL}/I_{dia}$). $I_{PL}$ represents the intensity of the defect related fluorescence, and $I_{dia}$ the intensity of the first order Raman signal, measured in the same conditions on the same diamond. These data can be deduced from spectra recorded in a spectral range overcoming the two signals and obtained using similar experimental conditions (*i.e.* same laser source).This parameter $I_{PL}/I_{dia}$, allows the direct comparison of the SiV PL emission of different diamonds discarding unique experimental conditions. Unfortunately, so far, not many papers have reported the spectra in the whole spectral range, including both the Raman and the color center peaks, but the authors believe that this parameter could be very representative especially when new methods to produce SiV in diamond are proposed.

In table 3 we present the $I_{PL}/I_{dia}$ ratios of diamonds reported in literature, in comparison with the diamonds synthitized in this work. As discussed previously, morphologically different diamonds are compared: thick film, thin film and single microcrystal/grain. The case of ultranano diamond films and powder has not been reported due to the very low and broad Raman signal, then a different approach should be developed to investigate these samples.

The whole spectra of our samples are reported in the supplementary information (S.I. Fig. 1, Fig.2, Fig.3 and Fig.4).

**Table 3**

| Sample | $I_{PL}/I_{dia}$ | Refs | Si source |
|---|---|---|---|
| Diamond thick film (thickness > 50 um) | 0.05 | [46] | From substrate |
| | 0.7 | [47] | |
| | 0.5 | [48] | |
| Diamond thin film (<5 um) | 11 | [49] | |
| | 17[a] | [50] | |
| | 12 | our sample without NiNP in S.I. Fig.1 | |
| | 150* | *our sample with NiNP in S.I. Fig.2 | |
| Microcrystals | 30 | [51] | |
| | 20 | Our sample without NiNP in S.I. Fig.3 | |
| | 250* | *our sample in S.I. Fig.4 | |

[a] Laser source at 488 nm,

Tab 3. col. 2 rows 1-7, reports $I_{PL}/I_{dia}$ of diamond films. Higher values are observed for thin films, thickness<5µm, (row4-7) respect to thick films, thickness>50µm, (row 1-3). This trend confirms the confinement of the SiV at the interface between the diamond film and the substrate, and the lower collection efficiency in thicker films. Furthermore we can speculate that the lower ratio values originate from a constant value of the SiV fluorescence in opposition with the increasing Raman intensities. The shielding effect of the growin film determines a limiting value in the number of defects formed during the synthesis and, consequently, in the fluorescence intensities.

Finally, the values of $I_{PL}/I_{dia}$ of isolated microcrystals, with size between 0.5 and 3 µm, are the largest among the three morphologies (col. 2 rows 7-10). These high values are due not

only to the lower contribution of the Raman signal to the ratio but also to the larger PL emission from small crystals compared to polycrystalline films. The presence of lattice defects and grain boundaries, characteristic of polycrystalline films, traps the photons emitted and determines a quenching of the fluorescence.Comparing the values of the $I_{PL}/I_{dia}$ of the diamonds obtained with our treatment to the ones found in literature, it is evident that the use of Ni NPs strongly improves the occurrence of SiV defects in diamond lattice enhancing the emission and the crystal quality of about 25 times, in the case of isolated micrograins and 10 times in the case of thin diamond films.

## 5. Conclusions

The proposed method is the first successful attempt to produce a massive amount of Si color centers in diamonds directly during the CVD growth without decreasing the crystal quality of the diamond lattice. A thermodynamic model was firstly developed to describe the mechanism of the Si inclusion in diamonds and a subsequent series of diamond synthesis was carried out to corroborate the model. The experimental results confirm the hypothesis made on the silicon inclusion. As predicted, the lowering of the surface tension of the silicon substrate due to the formation of nanosized Si-Ni compounds drives the formation of gaseous Si species. The formation of these species favors the inclusion of Si atoms in the growing diamonds, allowing the formation of massive SiV color centers. Thanks to this mechanism highly brilliant isolated single crystals or ultra-bright polycrystalline diamond films were synthetized. All the treatments with Ni NP are found to increase the Si related fluorescence compared to samples non-treated with Ni NP. Moreover, the samples treated with Ni NP show a faster growth respect to the substrates scratched with the only diamond paste. The observed catalytic effect of Ni particles to accelerate the formation of the diamond crystal is probably due to the higher surface/volume ratio of the seed-modified substrate. More interesting is the concomitant increase of the crystalline quality with the deposition rate associated with the use

of Ni NP. Such result undoubtedly deserves more investigations.The implementation of the deposition method of the Ni NP to confine the source of the Si gaseous species, as suggested by our results, could strongly improve the formation of localized ultra-bright diamond light sources for technological applications.

**References**


1. A. Gruber, A. Dräbenstedt, C. Tietz, L. Fleury, J. Wrachtrup, C. von Borczyskowski, *Science* 276, 2012–2014 (1997).
2. L. Childress, M. V. Gurudev Dutt, J. M. Taylor, A. S. Zibrov, F. Jelezko, J. Wrachtrup, P. R. Hemmer, and M. D. Lukin, *Science* 314, 281–285 (2006).
3. I. Aharonovich, S. Castelletto, D. A. Simpson, C-H Su, A. D. Greentree and S. Prawer, *Rep. Prog. Phys.* 74, 076501, (2011)
4. F. Jelezko, J. Wrachtrup, *New J. Phys*. 14,105024, (2012)
5. J. R. Rabeaua, A. Stacey, A. Rabeau, S. Prawer F. Jelezko, I. Mirza, J. Wrachtrup, *Nano Lett*, *7*, 3433–3437, (2007)
6. A.S. Barnard, *The Analyst*, 134*,* 1751, (2009)
7. A. Schrand, S.A. Ciftan Hens, O. Shenderova, *Critical Reviews in Solid State Materials Sciences,* 34, 18 (2009)
8. D. Le Sage, K. Arai, D. R. Glenn, S. J. DeVience, L. M. Pham, L. Rahn-Lee, M. D. Lukin, A. Yacoby, A. Komeili, R. L. Walsworth, *Nature,* 496, 486–489 (2013)
9. D. A. Simpson, A.D. Greentree, S. Prawer, I. Aharonovich, S. Castelletto, *Phys. Rev. A*, 81, 043813, (2010)
10. J. R. Rabeau, Y. L. Chin, S. Prawer F. Jelezko T. Gaebel J.Wrachtrup, *Applied Physics Letters*, 86, 131926, (2005)
11. V. S. Vavilov, A. A. Gippius, A. M. Zaitsev, B. V. Derjaguin, B. V. Spitsyn, A. E. Aleksenko *Sov. Phys.Semicond.* 14, 1078, (1981)

12. Clark C D, Kanda H, Kiflawi I and Sittas G 1995 *Phys. Rev.* B **51** 16681–88]
13. J. P. Goss, R. Jones, S. J. Breuer, P. R. Briddon, and S. Öberg, *Phys.Rev. Lett.* 77, 3041 (1996).
14. S. Moliver, *Tech. Phys.* 48, 1449 (2003)
15. K. Iakoubovskii, G Adriaenssens 2000 *Diam. Relat. Mater.* 9 1349,
16. E. Neu, M. Agio, C. Becher, Vol. 20, No. 18 *Optics Express* 19956.
17. Lachlan J. Rogers, Kay D. Jahnke, Marcus W. Doherty, Andreas Dietrich, Liam P. McGuinness, Christoph Müller, Tokuyuki Teraji, Hitoshi Sumiya, Junichi Isoya, Neil B. Manson, and Fedor Jelezko, *Phys. Rev. B* 89, 235101 (2014)
18. Tina Müller, Christian Hepp, Benjamin Pingault, Elke Neu, Stefan Gsell, Matthias Schreck, Hadwig Sternschulte, Doris Steinmüller-Nethl, Christoph Becher & Mete Atatüre, *Nature Communications* 5, 3328 (2014)
19. Ternschulte H, Thonke K, Sauer R, Münzinger P C and Michler P 1994 *Phys. Rev*. B 50 14554–60,
20. E. Neu, D. Steinmetz, J.Riedrich-Möller, S. Gsell, M. Fischer, M. Schreck, C. Becher, *New Journal of Physics* 13 (2011) 025012
21. Sébastien Pezzagna, Detlef Rogalla, Dominik Wildanger, Jan Meijer and Alexander Zaitsev, *New Journal of Physics* **13** (2011) 035024,
22. Aharonovich I, Castelletto S, Johnson B C, McCallum J C, Simpson D A, Greentree A D and Prawer S 2010 *Phys. Rev. B* 81 121201,
23. Chunlang Wang, Christian Kurtsiefer, Harald Weinfurter and Bernd Burchard, *J. Phys. B: At. Mol. Opt. Phys.* 39 (2006) 37–41
24. Grudinkin SA, Feoktistov N A, Medvedev A V, Bogdanov K V, Baranov A V, Vul' A Ya and Golubev V G, *J. Phys. D: Appl. Phys.* 45**,** 062001 (2012)

25. **S**. Orlanducci, V. Sessa, E. Tamburri, M.L. Terranova, M. Rossi, S. Botti, *Surface & Coatings Technology* , 201 (2007) 9389–9394

26. Terranova M.L, Piccirillo S, Sessa V, Botti S, Rossi M, *Appl. Phys. Lett.* 74, 3146 (1999)

27. May and M. N. R. Ashfold Yu. A. Mankelevich, *J. Appl. Phys.* 101, 053115 2007

28. James E. Butler, Richard L. Woodin, L. M. Brown and P. Fallon, Phil. *Trans. R. Soc. Lond. A* 1993 342, 209-224

29. E. Molinari, R. Polini, V. Sessa, M.L. Terranova and M. Tomellini (1993). *Journal of Materials Research*, 8, pp 785-797.

30. S.K. Kulkarni I, S.M. Gates , C.M. Greenlief and H. H. Sawin, *Surface Science* 239 (1990) 26-35

31. Stephen M. Gates, Roderick R. Kunz and C. Michael Greenlief, *Surface Science* 207 (1989) 364-384

32. Subhra Adhikari, N.N. Viswanathan, R.O. Dusane, *Journal of Non-Crystalline Solids* 352 (2006) 928–932

33. F. Comin, J. E. Rowe, P.H. Citrin, *Phys. Rev. Lett*. 51, 1983, 2404

34. B. Mutaftschiev, "The Atomistic Nature of Crystal Growth", Springer-Verlag Berlin Heidelberg New York 2001

35. M. Tinani, A. Mueller, Y. Gao, and E. A. Irene,Y. Z. Hu and S. P. Tay, *J. Vac. Sci. Technol. B* 19 (2) 2001, 376

36. Yu-Jeng Chang, J. L. Erskine, *Phys. Rev: B*, 28, 1983, 5766

37. S.Y. Tan, Chih-Wei Chen, I-Tse Chen, Chu-Wei Feng, *Thin Solid Films* 517 (2008) 1186–1190

38. G. Utlu, N. Artunc¸, S. Budak, S. Tari, *Applied Surface Science* 256 (2010) 5069–5075

39. S.L. Cheng, S.W. Lu, C.H. Li, Y.C. Chang, C.K. Huang, H. Chen, *Thin Solid Films* 494 (2006) 307 – 310

40. H.F. Yan, Y.J. Xing, Q.L. Hang, D.P. Yu, Y.P. Wang, J. Xu, Z.H. Xi, S.Q. Feng, *Chemical Physics Letters* 323 , 2000. 224–228

41. X.B. Zeng, Y.Y. Xu, S.B. Zhang, Z.H. Hu, H.W. Diao, Y.Q. Wang, G.L. Kong, X.B. Liao *Journal of Crystal Growth* 247 (2003) 13–16

42. E. Maillard-Schaller, B.I. Boyanov, S. English, R.J. Nemanich, *Mat.Res. Soc. Symp. Proc.* 514, 1998, 185,

43. Tomellini M., *J. Mater. Sci.* 43 (2008) 7102

44. Terranova M.L, Piccirillo S, Sessa V, Rossi M and Cappucci G, Adv. Mater, 5, 101 (1999)

45. Zaitsev, A. M. 2001 Optical properties of diamond. Springer.

46. M.G. Donato, G. Faggio, G. Messina, S. Santangelo, M. Marinelli, E. Milani, G. Pucella, G. Verona-Rinati, *Diamond and Related Materials* 13 (2004) 923–928

47. G. Dollinger, A. Bergmaier, C.M. Frey, M. Roesler, H. Verhoeven, *Diamond and Related Materials* 4, 1995, 591-595

48. K. Iakoubovskii, G.J. Adriaenssens, *Diamond and Related Materials* 9, 2000, 1349-1356

49. Igor I. Vlasov, Amanda S. Barnard, Victor G. Ralchenko, Oleg I. Lebedev, Mikhail V. Kanzyuba, Alexey V. Saveliev, Vitaly I. Konov, and Etienne Goovaerts *Adv. Mater.* 2009, 21, 808–812

50. S. W. Browd and S. C. Rand *J. Appl. Phys.* 78 (6), 15 September 1995, 4069

51. Alastair Stacey, Igor Aharonovich, Steven Prawer, James E. Butler, *Diamond & Related Materials* 18 (2009) 51–55

# Supplemetary information

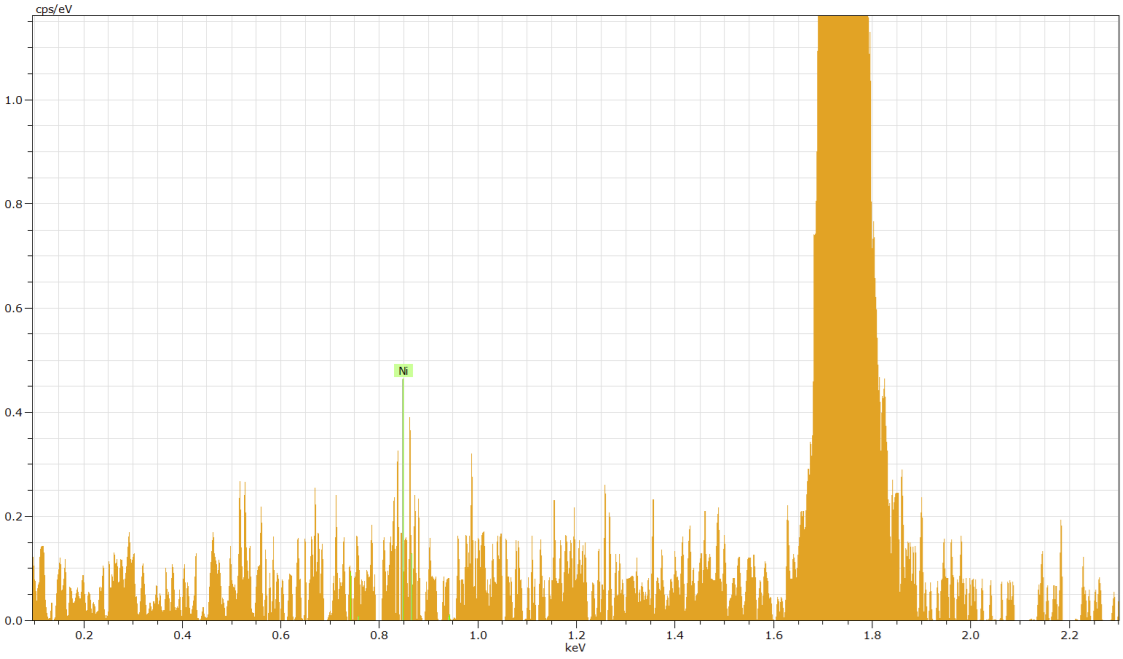


**a)**

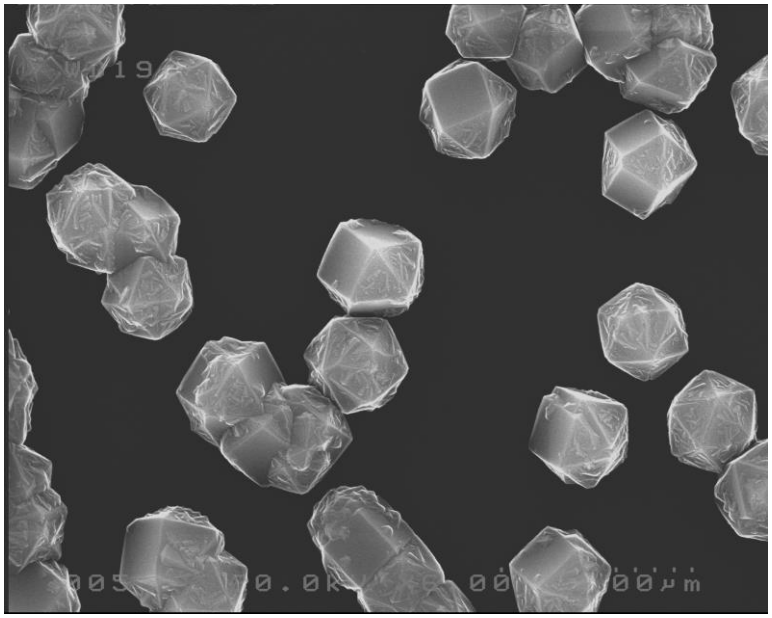

**b)**

Fig. 1 EDX a) from the reported SEM image b) of diamond crystall grown by using Ni NPs. A small peak due to Ni atoms is detected, the large band at about 1.75 keV come from the Si substrate

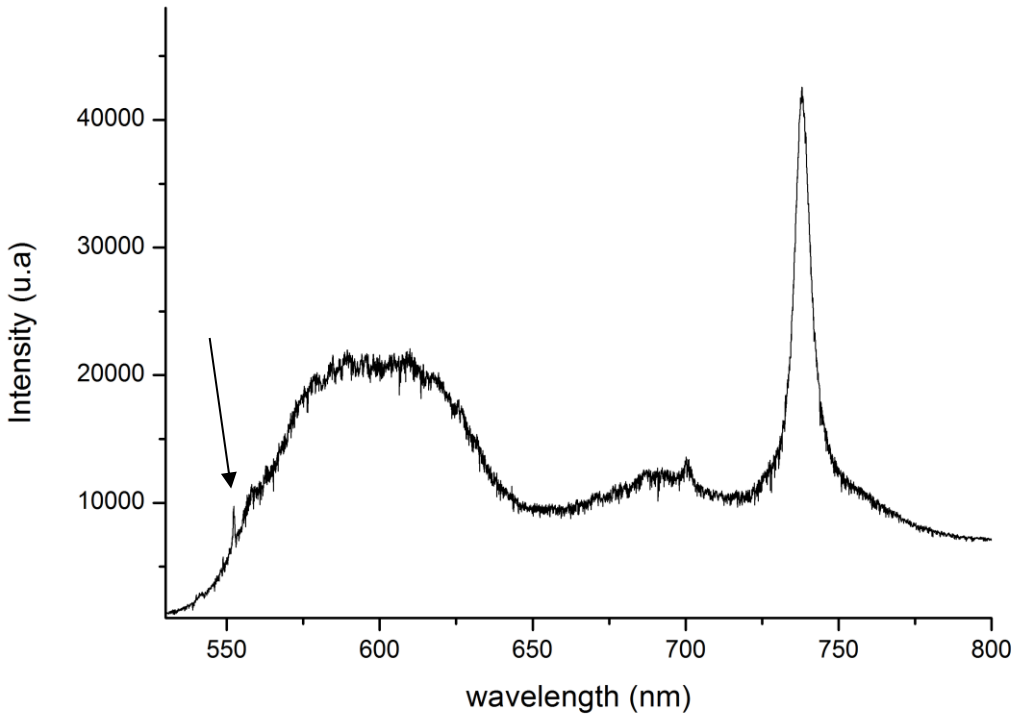


Fig.2 PL and Raman of CVD diamond film growth without Ni NP. The diamond Raman signal is indicated by the row.

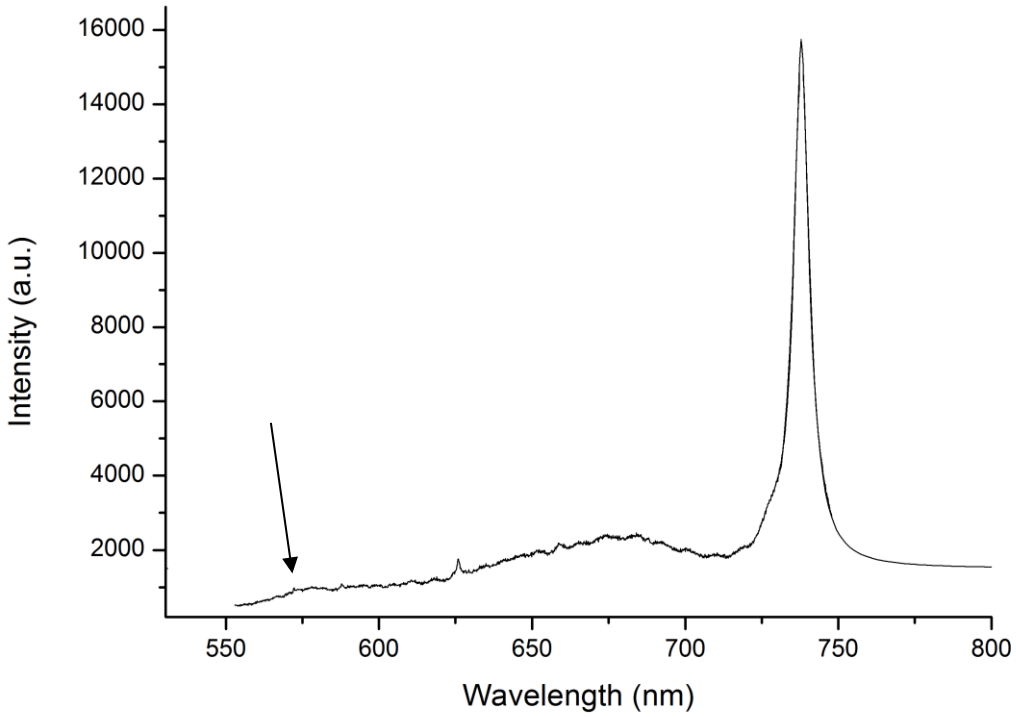

Fig.3 PL and Raman of CVD diamond film growth using Ni NP. The diamond Raman signal is signal is indicated by the row.

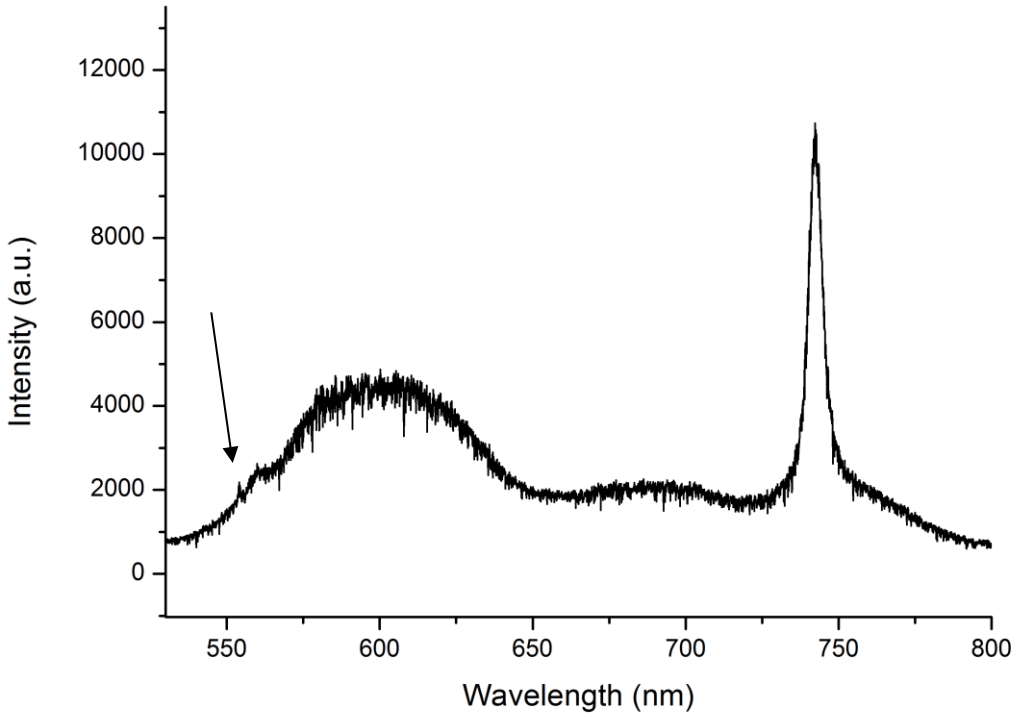


Fig. 4 PL and Raman of CVD diamond grains growth without Ni NP. The diamond Raman signal is signal is indicated by the row.

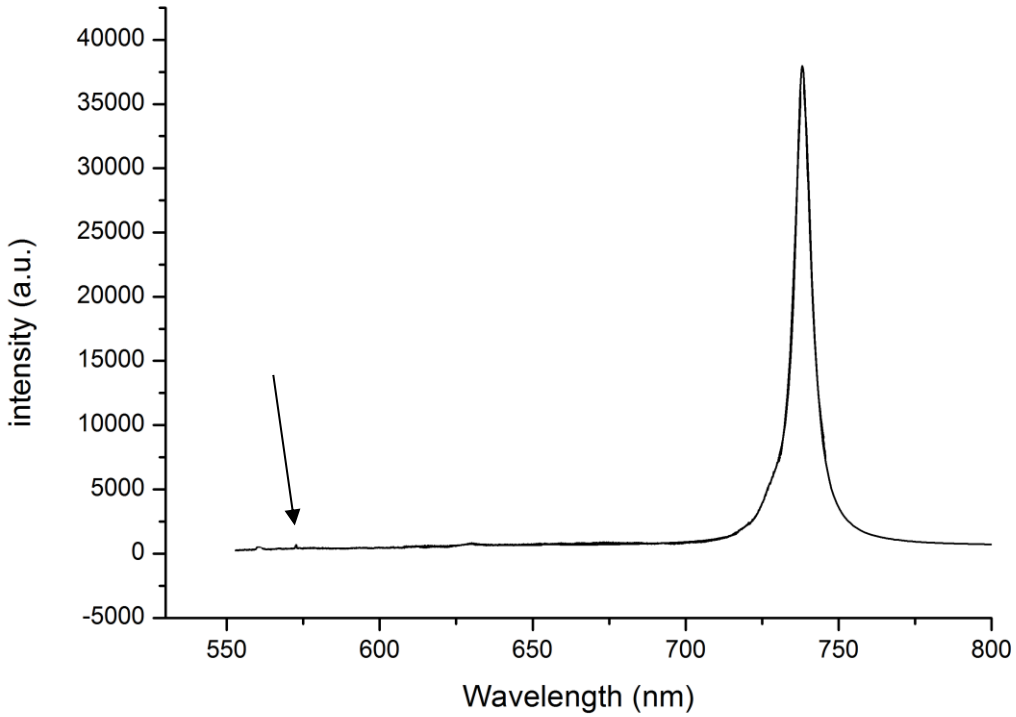


Fig. 5 PL and Raman of CVD diamond grains growth using Ni NP. The diamond Raman signal is signal is indicated by the row.

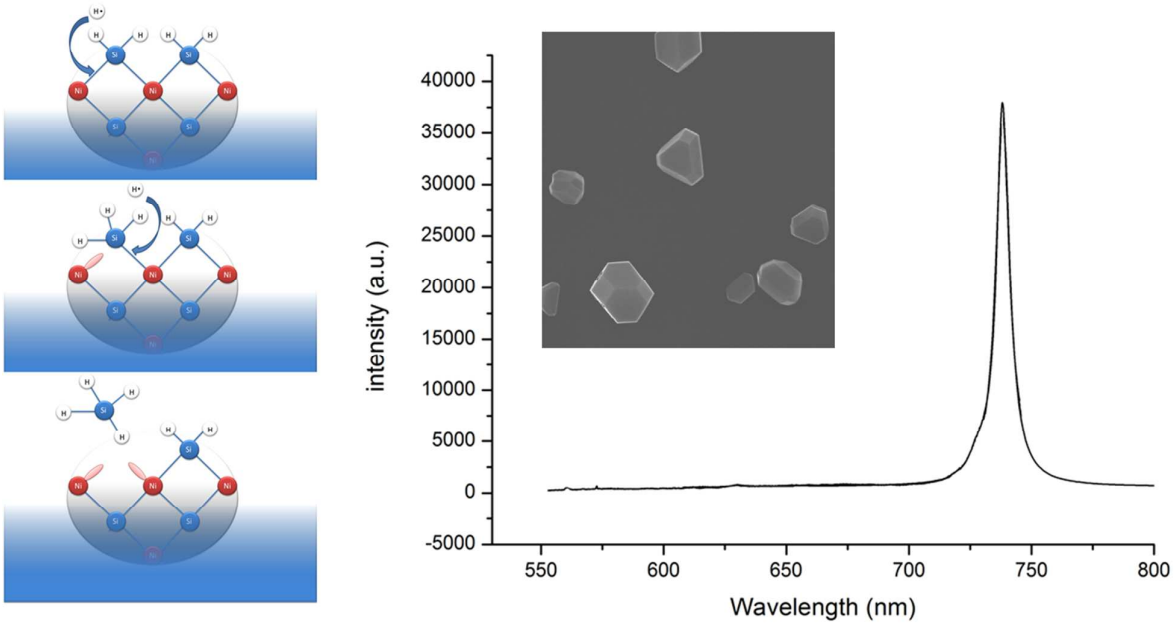


Nickel nanoparticles produce a massive amount of Si color centers in CVD diamonds